Air Data Estimation by Fusing Navigation System and Flight Control System

Chen Lu[1,2], Rong-Bing Li[1,2], Jian-Ye Liu[1,2] and Ting-Wan Lei[3]

[1](*Key Laboratory of Internet of Things and Control Technology in Jiangsu Province, Nanjing 20016, China*)
[2](*Navigation Research Center, College of Automation Engineering, Nanjing University of Aeronautics and Astronautics, Nanjing 210016, China*)
[3](*Chengdu Aircraft Design and Research Institute, Chengdu 610000, China*)
(E-mail: luchen@nuaa.edu.cn)

A novel synthetic air data estimation method without using air data sensors is presented, and the method only relies on the information from the Navigation System (NS) and Flight Control System (FCS). The aircraft's aerodynamic model is also required to make a connection between the FCS control parameters and the NS measurements. The airspeed, angle of attack and sideslip, angular velocity and wind speed are defined as state vectors, and state equations are established through the aircraft's aerodynamic model and dynamics. Linear velocity and angular velocity provided by the navigation system are considered as the measurement vector. To deal with variable wind fields, a novel Initialised Three-step Extended Kalman Filter (ITEKF), which considers the wind speed as an unknown input, is developed to track the variation of wind speed. Simulation results based on a Generic Hypersonic Vehicle (GHV) model are presented and compared with an existing method. Factors affecting the method's accuracy include the navigation system accuracy and the aerodynamic model error, are also discussed.

1. INTRODUCTION.   Air data, including airspeed, angle of attack and sideslip, indicate the force and heat conditions of the vehicle (Rohlf et al., 2004). Conventional Air Data Systems (ADS), which consist of a pitot-static subsystem and angle of attack vanes, are commonly used to accomplish air data sensing, measurement, calculation and output. The measurement accuracy and reliability of the air data system directly affects the performance of the Flight Control System (FCS). Thus, the capability of an ADS has a marked impact on flight safety, control efficiency and combat performance (Yadav et al., 2007). As basic

conditions for flight safety, the vehicle has to be equipped with a highly reliable and fault-tolerant ADS.

Recently, research into high mobility aircraft and hypersonic vehicles has markedly increased and such aircraft are beginning to come into service. These new types of vehicles make it difficult for air data measuring. High-speed manoeuvres cause large angles of attack and turbulent separation. Hypersonic and trans-atmospheric flight leads to stress on the structure and a high thermal environment. Considering the high performance of these vehicles (Guo et al., 2013), they will play an important role in space exploitation and in combat in the future (Wang et al., 2012). However, failure of a pressure-based ADS is a possibility under these specific external environmental conditions. (Baumann et al., 2008; Li et al., 2009). A redundant system would enhance the reliability and fault tolerance of the ADS (Westhelle, 2002).

Analytical redundancy means replacing the physical system with analytical models in safety-critical systems (Lie and Egziabher, 2013). As the physical hardware is replaced with a mathematical model, the reliable estimation of air data can be achieved with relatively low cost. Independent of traditional air data measurement devices, the analytical redundancy of an ADS eliminates the limits of installation location restrictions and airflow disturbance influences. Thus, this can apply to severe cases under which a pressure-based ADS could not work effectively, such as large angle of attack, high speed manoeuvring, trans-atmospheric flight and so on. In addition, the independence of the analytical redundant ADS from a pressure-based ADS has great advantages in many applications, not only providing a backup system for the traditional ADS but can also enhance the fault diagnosis and isolation capability for the traditional ADS. Hence, a model-based high-precision method to achieve reliable estimations of air data quantities is highly desirable. With available airborne information, a Virtual Air Data System (VADS) provides an air data measuring system independent of the existing ADS through an estimation algorithm.

In the early 1980s, a novel estimation method for attack angle and sideslip angle, which is not entirely dependent on air data sensors, was proposed to reconstruct re-entry air data parameters (Whitmore, 2002). Limited by the computing capacity, Zeis (1988) then proposed two self-governing estimators to calculate these two parameters separately, one for real-time estimation of attack angle and the other for real-time and post-flight estimation of sideslip angle. In the model of this estimator, air velocity, lift coefficient and Inertial Measurement Unit (IMU) measurements were used. Among them, the airspeed was provided by a traditional ADS. The estimation accuracy of attack and sideslip angle depended to a great degree on the precision of the lift coefficient model and the quality of IMU measurements. Based on this method, Myschik et al. (2008) utilised a complementary filter combined with an attack angle kinematics model to increase the system bandwidth. In combination with extended Kalman filtering theory, Wise (2013) used vehicle motion equations as state equations and estimated the angle of attack and sideslip with the pitch and roll angles from the Inertial Navigation System (INS) and the outputs of the IMU. This has proved the validity of using INS information or flight data to estimate angle of attack and sideslips.

The dynamic model of an air vehicle provides functions between the control surface deflections, air data parameters and the forces and moments acting on the vehicle. With the forces and moments known, the motion of the vehicle can be forecast using the vehicle dynamic model. Usually, this is provided by the navigation system. Thus, new thoughts, including aiding the navigation system with an aerodynamic model (Lyv et al., 2015;

Rhudy et al., 2013), estimating air data parameters using navigation information (Kampoon et al., 2015; Kargaard et al., 2015), and taking stock of an aerodynamic model based on the navigation parameters and air data (Chowdhary and Jategaonkar, 2010), have attracted considerable attention. As the ground speed (speed of the aircraft relative to geographic coordinates) is the vector sum of wind velocity and true air velocity, some researchers have estimated air data parameters after the wind speed estimation (Nebula et al., 2013; Cho et al., 2011).

Taking advantage of the relation between the dynamic model and air data parameters is a method of realising virtual air data estimation. Lie and Egziabher (2013) proposed a virtual air data estimation algorithm through two cascaded filters. The first filter processed integrated navigation of an INS and the Global Positioning System (GPS) and the second calculated the true air speed, wind velocity, angle of attack and sideslip with information from the first filter and a dynamic model of the vehicle. Compared with the previously mentioned methods, Lie and Egziabher's (2013) method has a distinct advantage in that it does not require the measurement of true air speed. Fravolini et al. (2012) realised the redundancy configuration and error detection of the ADS by adopting a similar virtual air data calculation scheme.

The dynamic model utilised in Lie and Egziabher (2013) relied on the hypothesis that the wind speed was constant, and the model was no longer exact under variations of wind speed. Moreover, their method considered the attitude parameters as a state vector, which were already calculated in the INS. Thus, the computation can be reduced through removing duplicate calculation.

Aiming at the development of a novel synthetic ADS under variable wind field with less computation than Lie and Egziabher (2013), an air data (including angle of attack, sideslip angle and true air velocity) estimation method fusing Navigation System (NS) and FCS is proposed in this paper. Taking the influence from a variable wind field into consideration, the dynamic model is established. The airspeed, angle of attack and sideslip as well as the angular velocity are designed as a state vector, and the state equation is derived. Considering the wind speed as an unknown input, an Initialised Three-step Extended Kalman Filter (ITEKF) is developed to obtain air data and wind speed under a variable wind field. Compared to the method in Lie and Egziabher (2013), the proposed method in this paper removes duplicated states (attitude angles) to achieve less computation and applies a novel filter to track the variation of wind speed.

The contributions of this paper are: (1) A new method for the estimation of air data with variable wind field is developed. The method only uses the output of navigation and flight control systems. (2) Comparison experiments with an existing method are conducted, and results show the proposed method performs better. (3) Experiments with or without a variable wind field are also done, and results with different sensor noise and aerodynamic model error are analysed.

The remainder of this paper is organised as follows. Section 2 describes air data modelling with the navigation system and a dynamic model. The relationship between the dynamic model and air data is illustrated first. Then, the mathematical connections among air data, ground speed and wind velocity are established. The novel air data estimation method, including filter model and method, is derived in Section 3, and simulation results are shown and discussed in Section 4. Concluding remarks are presented in Section 5.

2. AIR DATA MODELLING WITH NAVIGATION SYSTEM AND FLIGHT CON-
TROL SYSTEM. To develop the synthetic air data estimation method, air data modelling
with NS and FCS is essential. According to the aerodynamic model and the dynamic model,
a FCS changes flight attitude and motion parameters by control instructions generated on
account of the target and real-time attitude, velocity and position. The dynamic model of
the vehicle has been extensively studied. The aerodynamic model is well surveyed during
the design of the vehicle. To sum up, with these two models, the mathematical relationship
between air data, NS and FCS can be derived.

2.1. *Modelling of true air velocity, angle of attack and sideslip.* In this section, the
air data to be estimated is modelled according to the definition and the characteristics of
the wind field. Suppose the speed of the aircraft relative to navigation frame (North-East-
Down - NED frame) is $\vec{V}_G$ (ground speed), true air speed is $\vec{V}_T$, and wind speed is $\vec{V}_W$.
Hence, the following equation holds true:

$$\vec{V}_G = \vec{V}_T + \vec{V}_W \tag{1}$$

According to the relationship described in Figure 1, using the angle of attack α, sideslip
angle β and true air speed $\vec{V}_T$, the true air speed can be resolved into the body frame:

$$\begin{cases} U = V_T \cos\alpha \cos\beta \\ V = V_T \sin\beta \\ W = V_T \sin\alpha \cos\beta \end{cases} \tag{2}$$

where (U, V, W) are components of true air speed respectively aligned with the head, right
wing and the vertical direction of fuselage.

Rewriting Equation (1) into the body frame, we have

$$\begin{bmatrix} V_{Gx} \\ V_{Gy} \\ V_{Gz} \end{bmatrix} = \begin{bmatrix} U \\ V \\ W \end{bmatrix} + C_N^B \begin{bmatrix} V_{WN} \\ V_{WE} \\ 0 \end{bmatrix} \tag{3}$$

where (V_{Gx}, V_{Gy}, V_{Gz}) are components of $\vec{V}_G$ in the body frame, C_N^B is the attitude matrix
from navigation frame to body frame and (V_{WN}, V_{WE}) are north and east components of
wind speed.

As the ground speed far outweighs the turbulent velocity and its variation, and the time
flying over a long distance is very short, the change of the turbulent velocity is small enough
to be negligible (Cho et al., 2011). Taking this into consideration, the wind speed over a
short period of time can be regarded as constant, which means

$$\dot{V}_{WN} = \dot{V}_{WE} = 0. \tag{4}$$

2.2. *Aerodynamic modelling of air vehicle.* The forces and moments acting on the
vehicle come from the interaction on the vehicle of the speeding air flow. Thus, they are
inseparably linked with air data parameters. Following the modelling of true air veloc-
ity, angle of attack and sideslip, the aerodynamic model used to calculate the forces and
moments is discussed.

Structure parameters consist of mean aero chord $\bar{c}$, surface area of the wings S, span
of the wings B, reference centre of gravity as a fraction of mean aero chord X_{cgr}, centre
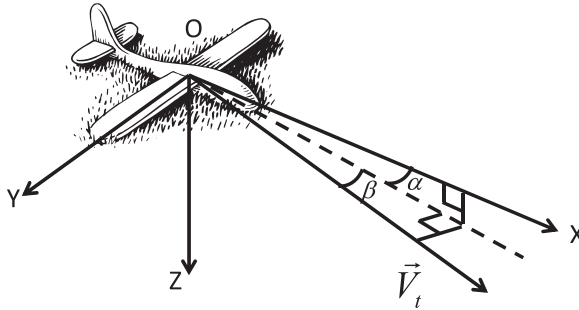
Figure 1.   Relation of angle of attack, angle of sideslip and true air speed.

of gravity as a fraction of mean aero chord X_{cg}, aerodynamic parameters, the moments of inertia and products of inertia of the air vehicle. Once the vehicle is designed, the structure parameters are known. Among them, the aerodynamic parameters under specific flight conditions are provided as tables. During flight, the real-time aerodynamic parameters can be achieved by table look-up and interpolations depending on designated parameters.

The integral force coefficients (C_{xt}, C_{yt}, C_{zt}) and moment coefficients (C_{lt}, C_{mt}, C_{nt}) of the aircraft can be calculated with the following equations:

$$(C_{xt}, C_{yt}, C_{zt}, (C_{lt}, C_{mt}, C_{nt})) = F_{ADC}(V_T, \alpha, \beta, P, Q, R, \delta_a, \delta_e, \delta_r) \tag{5}$$

where $(\delta_a, \delta_e, \delta_r)$ are the amount of rotation of the control surfaces, including aileron, elevator and rudder and (P, Q, R) are the angular velocities of the vehicle.

Based on the above integral force coefficients (C_{xt}, C_{yt}, C_{zt}) and the integral moment coefficients (C_{lt}, C_{mt}, C_{nt}), the forces and moments projected into the body coordinate, (F_x, F_y, F_z, L, M, N), can be calculated through:

$$\begin{cases} F_x = \bar{q}SC_{xt} + T, \quad F_y = \bar{q}SC_{yt}, \quad F_z = \bar{q}SC_{zt} \\ M_x = C_{lt}\bar{q}SB, \quad M_y = C_{mt}\bar{q}S\bar{c}, \quad M_z = C_{nt}\bar{q}SB \end{cases} \tag{6}$$

where T is engine gross thrust (decided by the throttle control information δ_T) and the dynamic pressure $\bar{q} = 0{\cdot}5\rho V_t^2$, in which ρ is the density of the air surrounding the vehicle. As the air density is a function of height, here we consider it as a known variable.

With Equations (5) and (6), $(F_x, F_y, F_z, M_x, M_y, M_z)$ become functions as:

$$(F_x, F_y, F_z, M_x, M_y, M_z) = F_{AD}(V_T, \alpha, \beta, P, Q, R, \delta_T, \delta_a, \delta_e, \delta_r) \tag{7}$$

2.3.   *Dynamic modelling of an air vehicle.*   With the forces and moments calculated, the motion of the air vehicle can be derived in the light of the dynamic model. The linear accelerations $\dot{U}, \dot{V}, \dot{W}$ and angular acceleration $\dot{P}, \dot{Q}, \dot{R}$ in the body coordinates can be

generated from the forces and moments through (Etkin, 2000):

$$
\begin{cases}
\dot{P} = \dfrac{J_z L + J_{xz} N - (J_z^2 - J_z J_y + J_{xz}^2)QR}{J_x J_z - J_{xz}^2} + \dfrac{J_{xz}(J_x - J_y + J_z)PQ}{J_x J_z - J_{xz}^2} \\[2ex]
\dot{Q} = \dfrac{M + (J_z - J_x)PR - J_{xz}(P^2 - R^2)}{J_y} \quad \dot{R} = \dfrac{J_{xz}L + J_x N + (J_x^2 - J_x J_y + J_{xz}^2)PQ}{J_x J_z - J_{xz}^2} \\[2ex]
\qquad - \dfrac{J_{xz}(J_x - J_y + J_z)QR}{J_x J_z - J_{xz}^2}
\end{cases}
\tag{8}
$$

$$
\begin{cases}
\dot{U} = RV - QW - g\sin\theta + F_x/m \\
\dot{V} = PW - RU + g\cos\theta\sin\phi + F_y/m \\
\dot{W} = QU - PV + g\cos\theta\cos\phi + F_z/m
\end{cases}.
\tag{9}
$$

where m is the mass of the air vehicle, g is the acceleration of gravity, θ is the pitch angle, ϕ is rotation angle and (J_x, J_y, J_z, J_{xz}) are the moment of inertia and product of inertia of the air vehicle.

Equation (9) is tenable under a constant wind field. Taking wind variation into consideration, the following model is derived according to the rigid body kinematics principle:

$$
\begin{bmatrix} \dot{V}_{Gx} \\ \dot{V}_{Gy} \\ \dot{V}_{Gz} \end{bmatrix}
=
\begin{bmatrix} 0 & R & -Q \\ -R & 0 & P \\ Q & -P & 0 \end{bmatrix}
\begin{bmatrix} V_{Gx} \\ V_{Gy} \\ V_{Gz} \end{bmatrix}
+
\begin{bmatrix} -\sin\theta \\ \cos\theta\sin\phi \\ \cos\theta\cos\phi \end{bmatrix} g
+ \frac{1}{m}
\begin{bmatrix} F_x \\ F_y \\ F_z \end{bmatrix}
\tag{10}
$$

where (V_{Gx}, V_{Gy}, V_{Gz}) are components of $\vec{V}_G$ in the body frame, C_N^B is an attitude matrix from navigation frame to body frame and (V_{WN}, V_{WE}) are north and east components of wind speed.

2.4. *Relationship of navigation system, flight control system to air data.* From Equations (7), (8) and (10), the relationship between NS, FCS and air data is achieved and shown in Figure 2. Based on the aerodynamic and dynamic models, the linear and angular accelerations $(\dot{V}_{gx}, \dot{V}_{gy}, \dot{V}_{gz}, \dot{P}, \dot{Q}, \dot{R})$ become functions of the control information $(\delta_T, \delta_a, \delta_e, \delta_r)$, the ground speeds (V_{gx}, V_{gy}, V_{gz}), the angular velocities (P, Q, R), the attitude angles (θ, ϕ) and the air data parameters (α, β, V_T). The control information is provided by the FCS, while the linear and angular velocities are measured by the NS. Hence, high precision estimation of air data can be achieved through fusing the information from the NS and FCS.

3. AIR DATA ESTIMATION METHOD. The relationship between the NS, the FCS and air data is analysed in Section 2, and a novel air data estimation method fusing the NS and FCS will be carried out in this section. The principle diagram of this method is shown in Figure 3. The filtering model for air data differs from that of Lie and Egziabher (2013), which used attitude angles as states, and attitude angles from the NS as measurements. Generally, attitude update is already completed in the INS navigation calculation and integrated navigation calculation. Using attitude angles as states means that the attitude update equations are repeated. On the other hand, the forces and moments calculated through the control parameters and aerodynamic model have a direct impact on the linear and angular velocities. Through the change of angular velocity, they indirectly affect the attitude. To ensure attack angle accuracy for the new types of vehicles, the positioning accuracy of the
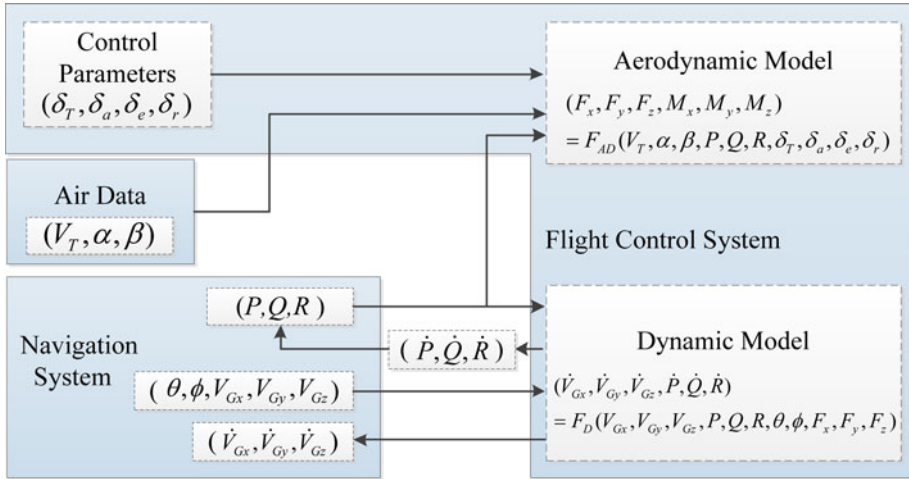
Figure 2.   Relationship of Navigation System, Flight Control System and air data.
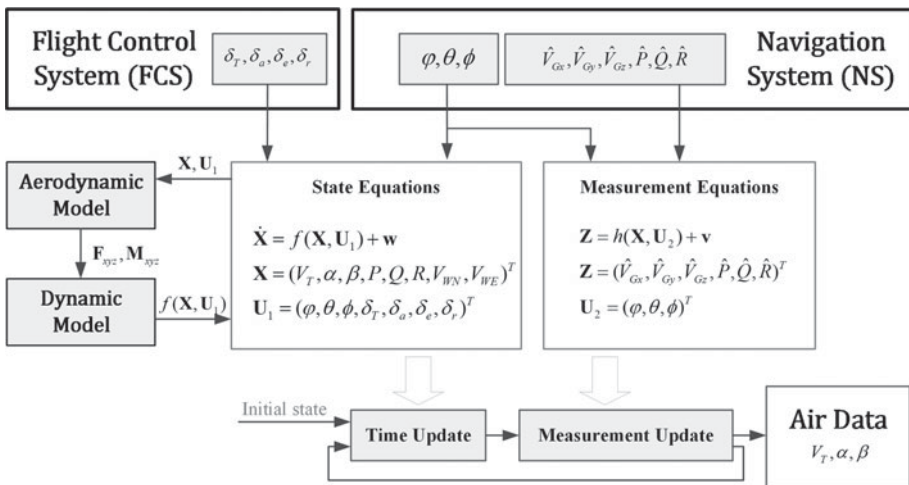

Figure 3.   Principle diagram of the calculation method for air data.

NS system has to achieve metre-level and the attitude accuracy should be arc-second level (Zhang et al., 2013). Thus, the attitude angles output from the NS are accurate enough to be used immediately. To avoid repeated calculation, air data, angular velocity and wind velocity are taken as the states to be estimated in this paper. The state equations are derived using the FCS control parameters and the aerodynamic and dynamic models. The NS provides all the measurements, including ground speeds and angular velocities. Details of the filtering model and method will be introduced in the following subsections.

   3.1.   *Equations of state.*   The state vector is defined as $\mathbf{X} = (V_T, \alpha, \beta, P, Q, R, V_{WN}, V_{WE})^T$ The state equation for $(P, Q, R, V_{WN}, V_{WE})$ can be obtained using Equations (8) and (4). The rest is the derivation of state equation of (V_T, α, β):

(1) Solve (V_{Gx}, V_{Gy}, V_{Gz}) with (V_T, α, β) and (V_{WN}, V_{WE}) through Equations (2) and (3).
(2) Solve $(\dot{V}_{Gx}, \dot{V}_{Gy}, \dot{V}_{Gz})$ with (V_{Gx}, V_{Gy}, V_{Gz}) through the aerodynamic model and the dynamic model, which are described in Equations (7) and (10).
(3) Obtain $(\dot{V}_T, \dot{\alpha}, \dot{\beta})$ with $(\dot{V}_{Gx}, \dot{V}_{Gy}, \dot{V}_{Gz})$ by differentiating Equation (2) as

$$\begin{bmatrix} \dot{V} \\ \dot{\alpha} \\ \dot{\beta} \end{bmatrix} = \begin{bmatrix} \cos\alpha\cos\beta & \sin\beta & \sin\alpha\cos\beta \\ \dfrac{-\sin\alpha}{V_t\cos\beta} & 0 & \dfrac{\cos\alpha}{V_t\cos\beta} \\ \dfrac{-\cos\alpha\sin\beta}{V_t} & \dfrac{\cos\beta}{V_t} & \dfrac{-\sin\alpha\sin\beta}{V_t} \end{bmatrix} \begin{bmatrix} \dot{U} \\ \dot{V} \\ \dot{W} \end{bmatrix} \tag{11}$$

where $(\dot{U}, \dot{V}, \dot{W})$ can be calculated through Equations (3) and (4) as follows

$$\begin{bmatrix} \dot{U} \\ \dot{V} \\ \dot{W} \end{bmatrix} = \begin{bmatrix} \dot{V}_{Gx}, \\ \dot{V}_{Gy}, \\ \dot{V}_{Gz} \end{bmatrix} + \begin{bmatrix} 0 & R & -Q \\ -R & 0 & P \\ Q & -P & 0 \end{bmatrix} \begin{bmatrix} V_{WN} \\ V_{WE} \\ 0 \end{bmatrix} \tag{12}$$

The state equation can be reorganised as

$$\dot{\mathbf{X}} = f(\mathbf{X}), \mathbf{U}_1 + \mathbf{w} \tag{13}$$

where $\mathbf{U}_1 = (\varphi, \theta, \phi, \delta_T, \delta_a, \delta_e, \delta_r)^T$ is the control input, including the attitude angle from the NS and flight control parameters from the FCS and $\mathbf{w}$ is gauss white noise of the system with the variance matrix $\mathbf{R}$.

3.2. *Measurement equations.* The measurement vector is defined as $\mathbf{Z} = (\hat{V}_{Gx}, \hat{V}_{Gy}, \hat{V}_{Gz}, \hat{P}, \hat{Q}, \hat{R})^T$, in which the variables are linear velocities and angular velocities from the NS. Usually real-time and high-accuracy navigation information can be obtained by fusing inertial navigation with GPS.

The measurement equations can be derived by Equation (3) as follows

$$\mathbf{Z} = h(\mathbf{X}, \mathbf{U}_2) + \mathbf{v} \tag{14}$$

$$h(\mathbf{X}, \mathbf{U}_2) = \begin{bmatrix} V_T\cos\alpha\cos\beta \\ V_T\sin\beta \\ V_T\sin\alpha\cos\beta \end{bmatrix} + C_N^B \begin{bmatrix} V_{WN} \\ V_{WE} \\ 0 \end{bmatrix} \tag{15}$$

where $\mathbf{U}_2 = (\varphi, \theta, \phi)^T$ is the control input, $\mathbf{v}$ is the noise of measurements, $\mathbf{Q}$ is the variance matrix of $\mathbf{v}$.

3.3. *Extended Kalman filter.* Considering the nonlinear character of the measurement equations, the Extended Kalman Filter (EKF) is applied to the state estimation problem of the dynamic model described by Equations (13) and (14). The nature of the EKF is minimum variance estimation following linearization and discretisation for nonlinear system through first-order Taylor approximation. Filter equations of the EKF are as follows:

$$\begin{cases} \hat{\mathbf{X}}_{k+1/k} = \hat{\mathbf{X}}_k + f(\hat{\mathbf{X}}_k, \mathbf{U}_{1,k}) \cdot \Delta T \\ \mathbf{P}_{k+1/k} = \mathbf{\Phi}_k \mathbf{P}_k \mathbf{\Phi}_k^T + \mathbf{Q} \\ \mathbf{K}_{k+1} = \mathbf{P}_{k+1/k} \mathbf{H}_{k+1}^T (\mathbf{H}_{k+1} \mathbf{P}_{k+1/k} \mathbf{H}_{k+1}^T + \mathbf{R}^{-1}) \\ \hat{\mathbf{X}}_{k+1} = \hat{\mathbf{X}}_{k+1/k} + \mathbf{K}_{k+1} \left\{ \mathbf{Z}_{k+1} - h(\hat{\mathbf{X}}_{k+1/k}, \mathbf{U}_{2,k+1}) \right\} \\ \mathbf{P}_{K+1} = (\mathbf{I} - \mathbf{K}_{k+1} \mathbf{H}_{k+1}) \mathbf{P}_{k+1/k} (\mathbf{I} - \mathbf{K}_{k+1} \mathbf{H}_{k+1})^T + \mathbf{K}_{k+1} \mathbf{R} \mathbf{K}_{k+1}^T \end{cases} \tag{16}$$

where k is the current time, $\hat{\mathbf{X}}_k$ is the optimal state estimation with the variance matrix $\mathbf{P}_k$, ΔT is the discrete time and $\mathbf{\Phi}_k$ and H_{k+1} are the Jacobian matrix of state equations and measurement equations respectively, which can be solved as

$$\mathbf{\Phi}_k = \mathbf{I} + \frac{\partial f(\hat{\mathbf{X}}_k, \mathbf{U}_{1,k})}{\partial \hat{\mathbf{X}}_k} \Delta T, \mathbf{H}_{k+1} = \frac{\partial h(\hat{\mathbf{X}}_{k+1/k}, \mathbf{U}_{2,k+1})}{\partial \hat{\mathbf{X}}_{k+1/k}} \tag{17}$$

where $\mathbf{I}$ is the identity matrix.

3.4. *Three-step Extended Kalman Filter.* In the above model, we consider the wind speed as constant. However, this is only tenable for a short time. Using the EKF algorithm to solve the filter model cannot track the wind variation. For this problem, a three-step EKF is adopted. A Three-step Kalman Filter (TKF) algorithm is used to obtain estimation with uncertain input in a dynamic system. It considers the uncertain inputs as unknown variables. The estimation of these unknown variables is added to a traditional Kalman Filter. Gillijns and Moor (2007) proposed a TKF for discrete linear systems. According to the principle of EKF, the Three-step Extended Kalman Filter (TEKF) is derived through the linearization of nonlinear systems in this paper.

First, dividing the state vector into two parts, $\mathbf{X} = (\mathbf{X}_1, \mathbf{X}_2)$, in which $\mathbf{X}_1 = (V_T, \alpha, \beta, P, Q, R)^T, \mathbf{X}_2 = (V_{WN}, V_{WE})^T \cdot \mathbf{X}_2$. is considered as unknown variables. The linearized model is achieved and given in the following pattern ($\mathbf{U}_1, \mathbf{U}_2$ are hidden for convenience):

$$\begin{aligned} \mathbf{X}_{1,k+1} &= \mathbf{X}_{1,k} + f_1(\mathbf{X}_{1,k}, \mathbf{X}_{2,k}) \cdot \Delta T + \mathbf{w}_1 \\ \mathbf{Z}_k &= h(\mathbf{X}_{1,k}, \mathbf{X}_{2,k}) + \mathbf{v} \end{aligned} \tag{18}$$

where $\mathbf{w}_1$ is gauss white noise and $\mathbf{Q}_1$ is the variance matrix of $\mathbf{w}_1$. We denote the Jacobian matrices of the nonlinear state and measurement equations as follows:

$$\mathbf{A}_k = \mathbf{I} + \frac{\partial f_1(\hat{\mathbf{X}}_{1,k}, \hat{\mathbf{X}}_{2,k})}{\partial \hat{\mathbf{X}}_{1,k}} \Delta T, \mathbf{G}_k = \mathbf{I} + \frac{\partial f_1(\hat{\mathbf{X}}_{1,k}, \hat{\mathbf{X}}_{2,k})}{\partial \hat{\mathbf{X}}_{2,k}} \cdot \Delta T$$

$$\mathbf{C}_k = \frac{\partial h(\hat{\mathbf{X}}_{1,k}, \hat{\mathbf{X}}_{2,k})}{\partial \hat{\mathbf{X}}_{1,k}}, \mathbf{H}_k = \frac{\partial f_1(\hat{\mathbf{X}}_{1,k}, \hat{\mathbf{X}}_{2,k})}{\partial \hat{\mathbf{X}}_{2,k}} \tag{19}$$

Thus, the calculation procedure of TEKF is

(1) Estimation of unknown input:

$$\tilde{\mathbf{R}}_k = \mathbf{C}_k \mathbf{P}_{1,k/k-1} \mathbf{C}_k^T + \mathbf{R}$$
$$\hat{\mathbf{X}}_{2,k} = (\mathbf{H}_K^T \tilde{\mathbf{R}}_K^{-1} \mathbf{H}_k)^{-1} \mathbf{H}_k^T \tilde{\mathbf{R}}_k^{-1} (\mathbf{Z}_k - h(\hat{\mathbf{X}}_{1,k/k-1}, 0)) \qquad (20)$$
$$\mathbf{P}_{2,k} = (\mathbf{H}_k^T \tilde{\mathbf{R}}_k^{-1} \mathbf{H}_k)^{-1}$$

(2) Measurement update:

$$\mathbf{K}_k = \mathbf{P}_{1,k/k-1} \mathbf{C}_k^T \tilde{\mathbf{R}}_k^{-1}$$
$$\hat{\mathbf{X}}_{1,k} = \hat{\mathbf{X}}_{1,k/k-1} + \mathbf{K}_k (\mathbf{Z}_k - h(\hat{\mathbf{X}}_{1,k}, \hat{\mathbf{X}}_{2,k}))$$
$$\mathbf{P}_{1,k} = \mathbf{P}_{1,k/k-1} - \mathbf{K}_k (\tilde{\mathbf{R}}_k - \mathbf{H}_k \mathbf{P}_{2,k} \mathbf{H}_k^T) \mathbf{K}_k^T \qquad (21)$$
$$\mathbf{P}_{12,k} = -\mathbf{K}_k \mathbf{H}_k \mathbf{P}_{2,k}$$

(3) Time update

$$\hat{\mathbf{X}}_{1,k+1/k} = \hat{\mathbf{X}}_{1,k} + f_1(\hat{\mathbf{X}}_{1,k}, \hat{\mathbf{X}}_{2,k}) \cdot \Delta T$$
$$\mathbf{P}_{1,k+1/k} = \begin{bmatrix} \mathbf{A}_k \\ \mathbf{G}_k \end{bmatrix} \begin{bmatrix} \mathbf{P}_{1,k} & \mathbf{P}_{12,k} \\ \mathbf{P}_{12,k}^T & \mathbf{P}_{2,k} \end{bmatrix} \begin{bmatrix} \mathbf{A}_k \\ \mathbf{G}_k \end{bmatrix} + \mathbf{Q}_1 \qquad (22)$$

As shown in the above steps, the time and measurement updates of the state estimation adopt the form of the standard Kalman filter. The unknown input is isolated, and its value is replaced by an optimal estimate in the TEKF.

3.5. *Initialised three-step extended Kalman filter.* Lu et al. (2016) points out that a TEKF is easily affected by the initial filtering error when applied to nonlinear filtering, subsequent experiments have verified this point. In this paper, an Initialised TEKF (ITEKF) algorithm is adopted. The EKF algorithm illustrated in Section 3.3 is used for filtering initialisation. When the filter is stabilised, the EKF algorithm can provide accurate initial estimates, and then switches to the TEKF algorithm. In this way, the accuracy of the TEKF algorithm can be ensured.

4. RESULTS AND DISCUSSION.

4.1. *Simulation test procedure.* For an air data estimation method based on information fusion of NS and FCS, the accuracy of estimated results is the key to verifying the feasibility and performance of the concept. The Generic Hypersonic Vehicle (GHV) aerodynamic model in Keshmiri and Colgren (2007) is used, and Equation (5) was used. After trimming the aircraft, we set the simulated vehicle flying under the three different conditions as shown in Table 1. Each flight lasts 30 seconds and the frequency of data was 10 Hz. We aimed to analyse the impact of measurement errors and a set of reference conditions shown in Table 2 was selected. In order to express the performance of the method proposed in this paper, the method in Lie and Egziabher (2013) was introduced and denoted as SADS2013 (Synthetic Air Data System 2013). The methods described in this paper are denoted as EKF, TEKF and ITEKF in accordance with the different filtering algorithms.

Table 1.   Flight condition.

Class	Description	Data
F1	steady wings-level flight	true air speed is 243·84 m/s
F2	steady turning flight	turning velocity is −2°/s
F3	steady pull-up flight	pull-up velocity is 1°/s

Table 2.   Reference measurement errors (mean square deviation).

Attitude angle	Linear velocity	Angular velocity	Control surface angles	Rate of max throttle
0·001°	0·1m/s	0·01°/s	0·1°	1%
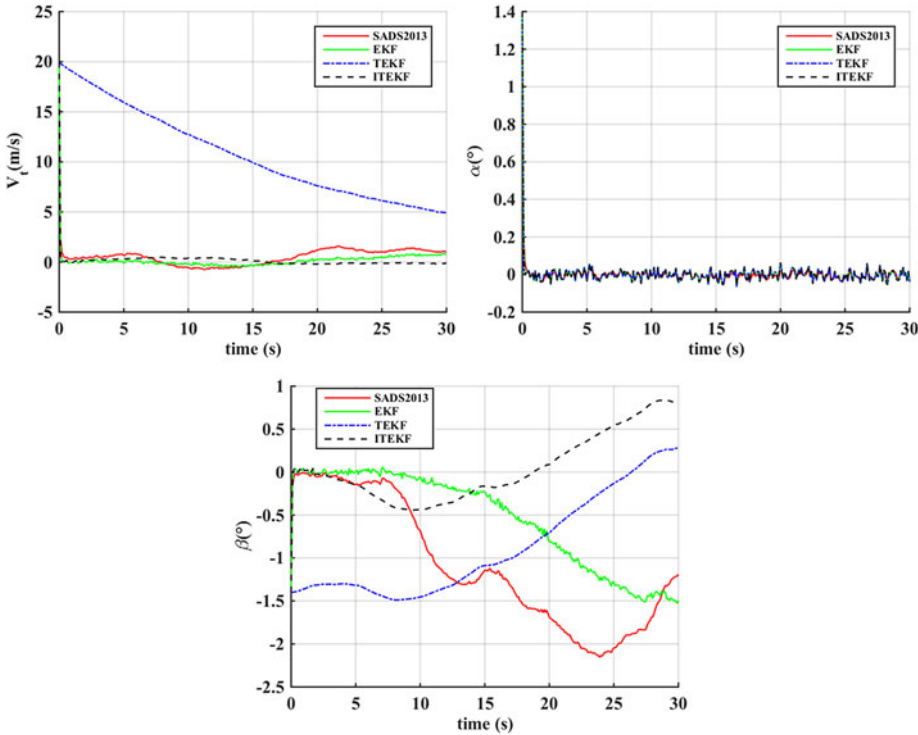
Figure 4.   Estimation error curves of airspeed, attack angle and sideslip angle.

4.2.   *Simulation results without wind field change.*   To analyse the performance of the above algorithms without a wind field change, simulation was conducted under flight condition F1 and the measurement errors in Table 2. The results of these algorithms are shown in Figure 4 and Figure 5. Figure 4 shows the estimation error curves of airspeed, attack angle and sideslip angle. Figure 5 plots the estimation error curves of wind speed.

The above figures depict that SADS2013, EKF and ITEKF can quickly converge to the real values in the presence of an initial estimation error, and the convergence rate is about the same. TEKF is easily affected by the initial estimation error. As the first step of TEKF is to estimate the uncertain input or state, a large initial state error will lead to a
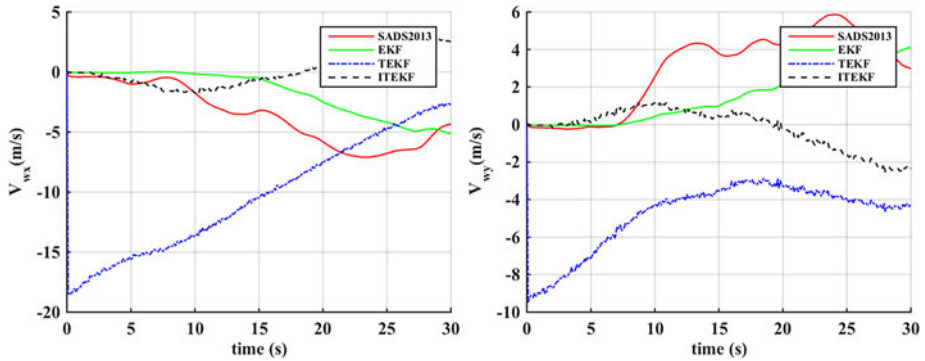
Figure 5. Estimation error curves of wind speed.

Table 3. Statistic characteristics of air data estimation errors.

	Mean (Standard Deviation)		
	SADS2013	EKF	ITEKF
V_T (m/s)	0·164 (1·305)	0·013 (1·200)	0·108 (1·164)
α $(°)$	0·004 (0·083)	0·005 (0·084)	0·005 (0·084)
β $(°)$	0·022 (1·051)	0·006 (0·443)	−0·002 (0·389)
V_{WN} (m/s)	0·052 (3·145)	0·079 (1·301)	−0·015 (1·160)
V_{WE} (m/s)	−0·114 (3·237)	0·011 (1·354)	−0·032 (1·150)

large estimation error of uncertain input or state (wind speed). It can be seen from the wind estimation error curves that, the errors of wind speed estimation through TEKF appear larger than other methods at the initial time. Although the errors gradually decrease during the following process of filtering, the convergence speed is too slow to provide effective filtering estimation.

Compared to SADS2013, EKF and ITEKF are more accurate at estimating true air velocity and sideslip angle. The accuracy of attack angle estimation is about the same. The reason is that SADS2013 uses three-axis components of true airspeed as state variables and then calculates air data. A relatively small error of the three-axis components of true airspeed will generate a large error of true air velocity, sideslip angle and attack angle in this way. The method proposed in this paper uses true air velocity, sideslip angle and attack angle as the state. The effect of the three-axis true airspeed components estimation error on the air data estimation accuracy is reduced through the filter.

In order to make the conclusion more convincing, 100 repetitions of Monte Carlo experiments under F1~F3 flight conditions were conducted. The estimation errors' statistical characteristics of SADS2013, EKF and ITEKF were calculated and are shown in Table 3. This shows that EKF and ITEKF are more accurate at estimating the true air velocity and sideslip angle than SADS2013, and the accuracy of the attack angle is about the same.

4.3. *Sensitivity to the sensor noise and aerodynamic model error.* Generally, the error of attitude is small, and the error in linear velocity is relatively large in the NS. Here the estimation errors under different linear velocity noise intensities are simulated and analysed. We set the noise intensity according to Table 2, 100 repetitions of Monte Carlo experiments
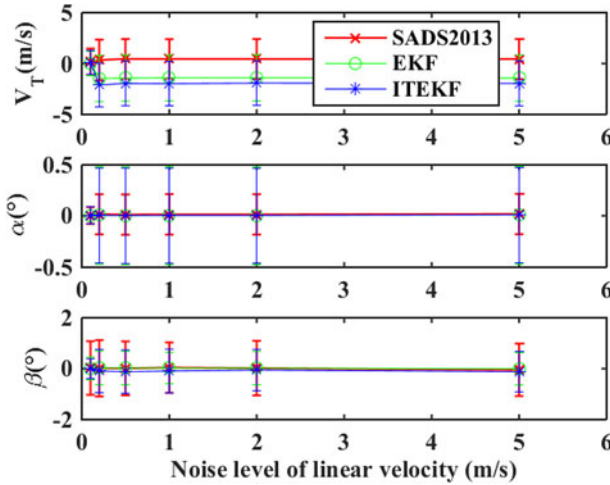
Figure 6.   Estimation errors under different linear velocity noise levels.

were conducted under F1∼F3 flight conditions. Then, we increased the linear velocity noise level and conducted more simulations in the same way. Simulation results are plotted in Figure 6. Results indicate that the filter can still achieve good estimation accuracy when the mean square deviation of the linear velocity measurement noise is increased to 5 m/s. This result is consistent with the filtering model. The influencing factors of the estimation of the state come from two parts: the aerodynamic and dynamic model in the state update and the linear and angular velocities in the measurement update. When the linear velocities contain large noises, the filter will calculate the state depending more on the state update and measurement update of angular velocities. Hence, the accuracy of state estimation can be ensured.

The aerodynamic model plays an indispensable role in the air data estimation. Through adding noise to the aerodynamic coefficients, the influence of an inaccurate aerodynamic model to the estimation performance was analysed. Noises at different percentages of the accurate aerodynamic coefficients were added separately. The mean and standard deviation of the errors are shown in Figure 7. The result shows that the filter can provide air data estimation with enough accuracy even if the error intensity of the aerodynamic coefficient is increased to 15%.

4.4.   *Simulation results with wind field change.*   The performance of the air data estimation methods with wind field change is tested in this section. The estimation errors of air data achieved through SADS2013, EKF, TEKF and ITEKF are shown in Figure 8. The wind speed estimation errors are shown in Figure 9, in which REFERENCE means the wind field set in the simulation. As shown in Figure 9, the X-component of wind speed is gradually changed from 10 s to 15 s, and the Y-component remains unchanged. SADS2013 and EKF have the trend to track the wind change; only ITEKF can track the wind change effectively and quickly; TEKF has a relatively larger initial deviation as a result of the initial estimation error, the subsequent estimation is highly influenced by the initial deviation. The conclusion can be drawn that ITEKF has the ability to track high-speed wind field change.
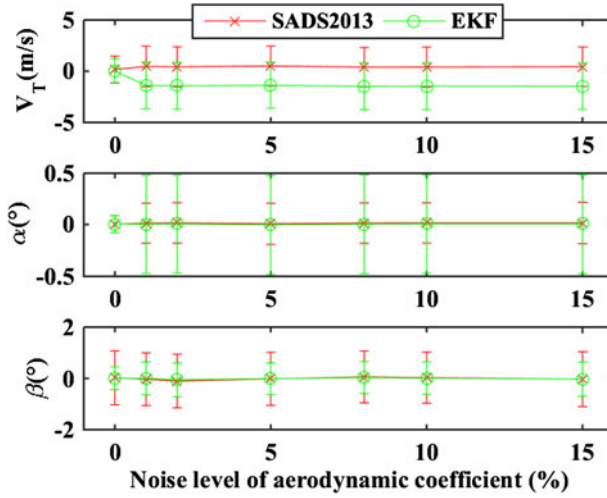
Figure 7.   Estimation errors under different aerodynamic coefficient noise levels.
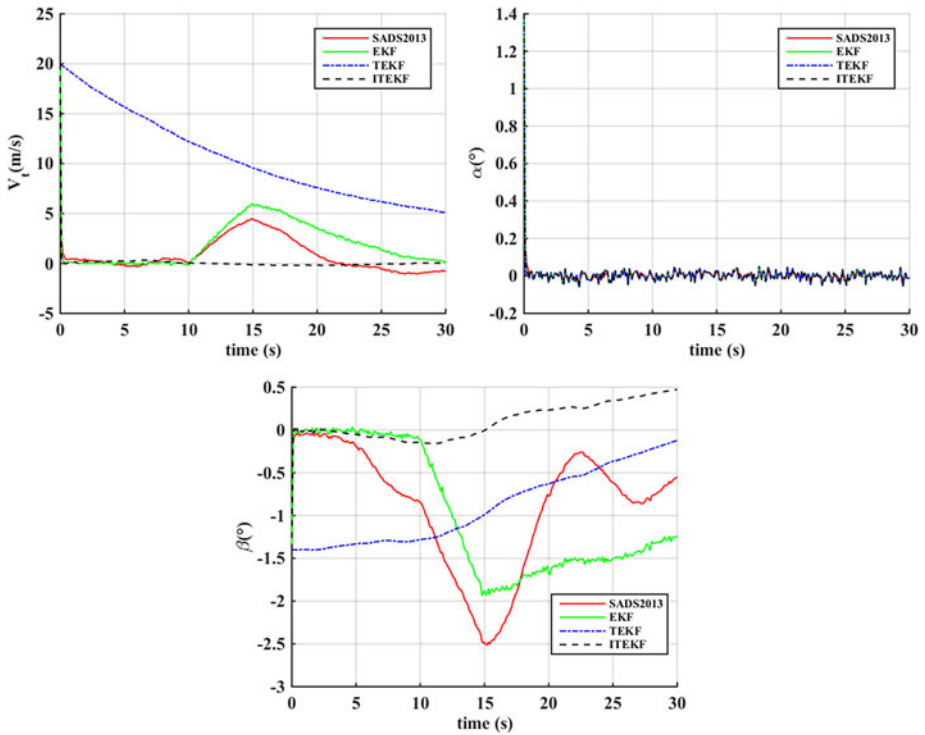

Figure 8.   Air data estimation errors with variable wind field.
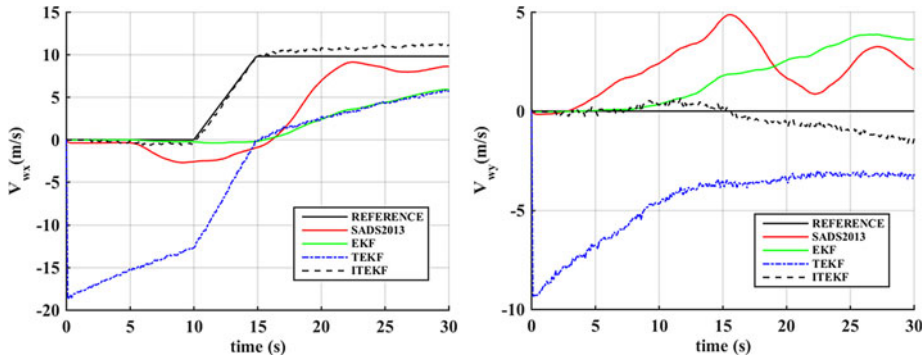
Figure 9.   Estimation of wind speed with variable wind field.

5. CONCLUSION. This paper presents a novel air data estimation method based on information from the navigation system, flight control system and the aircraft's aerodynamic model. The method shows good performance on simulated flight data, even under large navigation and aerodynamic model errors. A novel nonlinear Kalman filter method is proposed, and the filter appears to be insensitive to initial estimation error and shows good tracking performance of a variable wind field. It is judged that the proposed method in this paper is able to provide analytical redundancy or backup to a traditional air data system.

ACKNOWLEDGEMENTS

REFERENCES

Baumann, E., Pahle J., Davis M. and White J. (2008). X-43A Flush Air Data Sensing System Flight-test Results. *Journal of Spacecraft and Rockets*, **47**(1), 48–61.

Cho, A., Kim, J., Lee, S. and Kee, C. (2011). Wind Estimation and Airspeed Calibration Using a UAV with a Single-Antenna GPS Receiver and Pitot Tube. *IEEE Transactions on Aerospace and Electronic Systems*, **47**(1), 109–117.

Chowdhary, G. and Jategaonkar, R. (2010). Aerodynamic Parameter Estimation from Flight Data Applying Extended and Unscented Kalman Filter. *Aerospace Science and Technology*, 14 (2), 106–117.

Etkin, B. (2000). *Dynamics of Atmospheric Flight*. Dover Publications, New York, US.

Fravolini, M.L., Pastorelli, M., Pagnottelli, S., Valigi, P., Gururajan, S., Chao, H. and Napolitano, M.R. (2012). Model-Based Approaches for the Airspeed Estimation and Fault Monitoring of an Unmanned Aerial Vehicle. *IEEE Workshop on Environmental Energy & Structural Monitoring Systems (EESMS)*, 18–23.

Gillijns, S. and Moor, B.D. (2007). Unbiased Minimum-Variance Input and State Estimation for Linear Discrete-Time Systems with Direct Feedthrough. *Automatica*, **43**, 934–937.

Guo, J.F., Fu, Y. and Cui, N.G. (2013). Three-Dimensional Autonomous Entry Guidance Method. *Control and Decision*, **28**(5), 688–694.

Kampoon, J.W., Okolo, W., Erturk, S.A., Daskiran, O. and Dogan, A. (2015). Wind Field Estimation and Its Utilization in Trajectory Prediction. *AIAA SciTech Forum*, 1–26.

Kargaard, C.D., Kutty, P. and Schoenenberger, M. (2015). Coupled Inertial Navigation and Flush Air Data Sensing Algorithm for Atmosphere Estimation. *AIAA Atmospheric Flight Mechanics Conference, AIAA SciTech Forum*, 1–18.

Keshmiri, S. and Colgren, R. (2007). Six DoF Nonlinear Equations of Motion for a Generic Hypersonic Vehicle. *AIAA Atmospheric Flight Mechanics Conference and Exhibit*, 1–29.

Li, Q.D., Chen, L.L. and Zhang, X.G. (2009). Flush Airdata Sensing System Fast Intelligent Fault Detection and Diagnosis Technology. *Systems Engineering and Electronics*, **31**(10), 2544–2546.

Lie, F.A.P. and Egziabher, D.G. (2013). Synthetic Air Data System. *Journal of Aircraft*, **50**(4), 1234–1249.

Lu, P., Eykeren, L.V., Kampen, E.V., Visser, C.C.D. and Chu, Q.P. (2016). Adaptive Three-Step Kalman Filter for Air Data Sensor Fault Detection and Diagnosis. *Journal of Guidance, Control, and Dynamics*, **39**(3), 590–604.

Lyv, P., Lai, J.Z., Liu, J.Y., Zhu, B., and Song, Y.F. (2015). Overview and Progress on Study of Aircraft Aerodynamics Model Aided Navigation Method. *Control and Decision*, **30**(11), 1–7.

Myschik, S., Holzapfel, F. and Sachs G. (2008). Low-Cost Sensor Based Integrated Airdata and Navigation System for General Aviation Aircraft. *Proceedings of AIAA Guidance Navigation and Control Conference and Exhibit*, 1–21.

Nebula, F., Palumbo, R. and Morani, G. (2013). Virtual Air Data: a Fault-Tolerant Approach Against ADS Failures. *AIAA Infotech at Aerospace Conference*. 1–14.

Rhudy, M., Larrabee, T., Chao, H.Y., Gu, Y. and Napolitano, M.R. (2013). UAV Attitude, Heading, and Wind Estimation Using GPS/INS and an Air Data System. *AIAA Guidance, Navigation, and Control Conference*, 1–11.

Rohlf, D., Brieger, O. and Grohs, T. (2004). X-31 VECTOR System Identification Approach and Results. *AIAA Atmospheric Flight Mechanics Conference and Exhibit*, 1–12.

Wang, Y.F., Wu, Q.X., Jiang, C.S. and Zhang, Q. (2012). Multi-model Switching Control for Near Space Vehicle. *Control and Decision*, **27**(10), 1452–1458.

Westhelle, C.H. (2002). X-38 Backup Air Data System (AeroDAD). *40th AIAA Aerospace Sciences Meeting and Exhibit*, 1–12.

Whitmore, S.A. (2002). Reconstruction of the Shuttle Reentry Air Data Parameters Using a Linearized Kalman Filter. *AIAA Atmospheric Flight Mechanics Conference*, 1–13.

Wise, K.A. (2013). Flight Testing of the X-45A J-UCAS Computational Alpha-Beta System. *AIAA Guidance, Navigation, and Control Conference and Exhibit*, 1–14.

Yadav, V., Padhi, R. and Balakrishnan, S.N. (2007). Robust/Optimal Temperature Profile Control of a High-Speed Aerospace Vehicle Using Neural Networks. *IEEE Transactions on Neural Networks*, **18**(4), 1115–1128.

Zhang, C., Xiong, Z., Wang, R., Liu, J.Y. and Peng, H. (2013). New INS/CNS Integrated Algorithm On Aerospace Vehicle with Directly Sensing Horizon. *Chinese Space Science and Technology*, **3**, 64–71.

Zeis, J.E. (1988). *Angle-of-Attack and Sideslip Estimation Using Inertial Reference Platform*. Air Force Institute of Technology, Wright-Patterson Air Force Base, 80–84.